# Effects of phonon bandgap on phonon–phonon scattering in ultrahigh thermal conductivity $\theta$-phase TaN

Chao Wu(吴超)[1,4] and Chenhan Liu(刘晨晗)[1,2,3,†]

[1] *Laboratory of Solid State Microstructures, Nanjing University, Nanjing* 210093, *China*
[2] *Micro- and Nano-scale Thermal Measurement and Thermal Management Laboratory, School of Energy and Mechanical Engineering, Nanjing Normal University, Nanjing* 210023, *China*
[3] *Jiangsu Key Laboratory for Numerical Simulation of Large-Scale Complex Systems, Nanjing Normal University, Nanjing* 210023, *China*
[4] *Jiangsu Key Laboratory for Design and Manufacture of Micro-Nano Biomedical Instruments, School of Mechanical Engineering, Southeast University, Nanjing* 211100, *China*

(Received 16 November 2022; revised manuscript received 6 January 2023; accepted manuscript online 11 January 2023)

Phonon bandgap typically has a significant effect on phonon–phonon scattering process. In this work, the effects of mass modified phonon bandgap in $\theta$-phase TaN are systemically investigated by the means of first-principles calculations with linearized Boltzmann transport equation. Through detailed calculations, we find that phonon bandgap has a significant effect on three-phonon process while exhibits a much weaker effect on four-phonon process. The reason for the ultrahigh thermal conductivity of $\theta$-phase TaN is the long lifetime of phonons including both three-phonon and four-phonon processes, which originates from the weak phonon anharmonicity and large phonon bandgap-induced small phonon–phonon scattering phase space. This work advances the understanding of phonon bandgap effects on phonon transport.

**Keywords:** ultrahigh thermal conductivity, phonon–phonon scattering phase space, first-principles calculation, phonon bandgap

**PACS:** 65.40.–b, 63.20.kg, 63.20.dk, 63.20.D– **DOI:** 10.1088/1674-1056/acb201

## 1. Introduction

With the progressively shrinking size of transistors in integrated circuits, optimizing the heat dissipation in nanoscale electronic and optoelectronic devices is an emerging challenge. Thus, the ultrahigh thermal conductivity materials, due to their outstanding heat conduction ability, are attracting more and more attention in the field of heat management. For example, in 2018, three *Science* papers were published at the same day to report the ultrahigh thermal conductivity material BAs.[1–3] For the theory history of searching high thermal conductivity, Slack's rules were raised first in 1973[4] and graphene[5,6] and diamond[7–9] are the two famous examples to show the ability of these rules. Then in 2013, two new selection rules, including large acoustic–optical phonon frequency gap (phonon bandgap) and bunching of the acoustic phonon branches (acoustic bunching), that restrain phonon–phonon scattering strength were proposed.[10] The discovery of BAs[1–3,11] verifies the ability of the two rules. Recently, crystal symmetry was found to have a significant effect on the thermal conductivity,[12–14] which was also employed for ultrahigh thermal conductivity.[15]

Based on the two selection rules proposed in 2013, recently, $\theta$-TaN was theoretically predicted to have a high thermal conductivity of 995 W/(m·K) at room temperature.[16] Through detailed first-principles calculations, phonons are the main heat carriers in $\theta$-TaN and its ultrahigh thermal conductivity is originated from several couple of factors: large phonon bandgap, acoustic bunching, low isotopic scattering, and weak electron–phonon scattering. The theoretical prediction of $\theta$-TaN further verifies the ability of the two selection rules for searching ultrahigh thermal conductivity. However, although the two selection rules predicted the ultrahigh thermal conductivity of $\theta$-TaN, it is still unclear that how the magnitude of thermal conductivity and phonon–phonon scattering strength varies with the phonon bandgap. For monolayer graphene, without any phonon bandgap, recent first-principles calculations observed the giant enhancement of phonon–phonon scattering strength and decrease of thermal conductivity if four-phonon process is included.[17–19] Thus, it is necessary to investigate the effects of phonon bandgap on the phonon–phonon scattering strength of three-phonon and four-phonon processes (Fig. 1) for $\theta$-TaN.

In this work, by the means of first-principles calculations with linearized Boltzmann transport equation,[20–24] we systematically investigate the thermal conductivity of $X$N ($X$ is Ta, Nb, and V). Through modifying the phonon bandgap of $\theta$-TaN by replacing Ta with Nb and V, we find that the phonon bandgap has a significant effect on the phonon–phonon scattering phase space of three-phonon process (P3) while has a much weaker effect on the phonon–phonon scattering phase space of four-phonon process (P4). For NbN and VN, the phonon bandgap has a weak effect on their P3, P4, and thermal conductivity. This work advances the understanding of the effects of phonon bandgap on the phonon–phonon scattering and

†Corresponding author. E-mail: chenhanliu@njnu.edu.cn

© 2023 Chinese Physical Society and IOP Publishing Ltd 

explores the possibility of TaN in thermal management.[25–27]

## 2. Results and discussion

Figure 1 shows the atomic structures of *X*N. All the three materials have the same crystal symmetry with the space group of *P*-6*m*2 (No. 187), which can exclude the effects of crystal symmetry since crystal symmetry can significantly affect the phonon–phonon scattering strength and thermal conductivity.[12,14,15] The lattice structure information of the three materials is shown in Table 1. From the table, VN has the shortest bond length V–N. Combining the lightest mass of V, VN has the largest phonon group velocity (Fig. 2(a)) compared with NbN (Fig. 2(e)) and TaN (Fig. 2(i)). NbN and TaN have similar bond length, thus, NbN should have larger phonon group velocity than TaN due to the lighter mass of Nb.

**Table 1.** Lattice structure information of *X*N.

| *X*N | *a* (Å) | *b* (Å) | *c* (Å) | *γ* (°) | *X*–N bond length (Å) | Reference |
|---|---|---|---|---|---|---|
| VN | 2.712 | 2.712 | 2.624 | 120 | 2.043 | |
| NbN | 2.934 | 2.934 | 2.856 | 120 | 2.215 | this work |
| TaN | 2.926 | 2.926 | 2.873 | 120 | 2.218 | |
| | 2.936 | 2.936 | 2.885 | 120 | – | Expt.[28] |

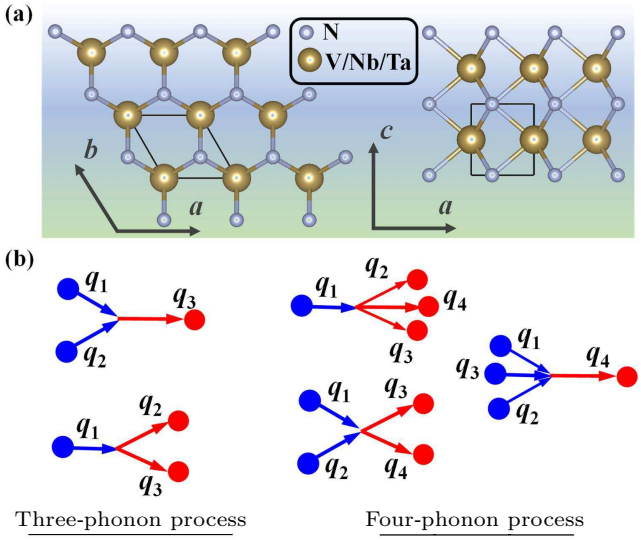



**Fig. 1.** (a) Atomic structures of *X*N. The solid black lines indicate the primitive unit cell. (b) Schematic diagram of three-phonon and four-phonon processes. $q_j$ ($j = 1$–4) means the phonon mode.

Figure 2 shows the phonon dispersions of VN (a), NbN (e), and TaN (i). Due to the largest mass difference, the phonon bandgap of TaN is largest (7.6 THz). And the phonon bandgap in NbN (4.1 THz) and VN (2.9 THz) is much smaller. Importantly, the phonon bandgap in TaN is almost identical to the maximum frequency $\omega_{a,max}$ (8.1 THz) of acoustic phonons, inhibiting the three-phonon process. While in NbN and VN, $\omega_{a,max}$ is much larger due to the lighter mass of Nb and V and their phonon bandgap is much smaller than the corresponding $\omega_{a,max}$, making the three-phonon process much easier to happen. Since the mass of *X* in *X*N has a significant effect on phonon bandgap, in order to realize the modification of phonon bandgap, replacing *X* with a different mass is introduced. As shown in Figs. 2(a)–2(c), 2(d)–2(f), and 2(h)–2(i), when force constant is fixed, the phonon bandgap increases monotonously with increasing the mass of atom *X* (V, Nb, or Ta). For example, with *X* increasing from V to Ta, the phonon bandgap for fixed force constant $k_{TaN}$ increases from 1.0 THz to 7.6 THz or 0 THz to 6.0 THz. Interestingly, the mass of *X* only affects the acoustic branches while the optical branches almost have no change. That is reasonable since for two-atom primitive unit cell, heavy atom dominates the low-frequency phonons and light atom dominates the high-frequency phonons. There are 2 atoms in the primitive unit cell of *X*N, *i.e.*, six branches in the phonon dispersion, thus three (acoustic) branches are dominated by the heavy *X* atom and the other three (optical) branches are dominated by the light N atom. Modifying the mass of *X* can significantly modify the *X* dominated acoustic branches.

Through carefully comparing the nine phonon dispersions in Fig. 2, the phonon dispersion or the phonon bandgap has a significant change if modifying the mass of *X* with fixed force constant, while only has a slight change if modifying force constant with fixed mass of *X*. For example, the phonon dispersion of "$k_{NbN}$–$m_{NbN}$" (Fig. 2(e)) is similar to that of "$k_{TaN}$-$m_{NbN}$" (Fig. 2(h)) while is much different to that of "$k_{NbN}$-$m_{VN}$" (Fig. 2(d)). Thus, the force constants among TaN, NbN, and VN are similar while their masses are much different. Such different phenomena of mass and force constant dependent phonon dispersion are also distinctly indicated by the phonon density of states (DOS) as shown in Fig. 3. To be more specific, the phonon DOS shape of "$k_{TaN}$–$m_{NbN}$" is very similar to that of "$k_{NbN}$–$m_{NbN}$" while is much different to that of "$k_{TaN}$–$m_{VN}$". From the phonon DOS, we can also obtain that "$k_{TaN}$–$m_{TaN}$" has the largest the phonon bandgap and "$k_{VN}$–$m_{VN}$" has the smallest phonon bandgap. With the mass decreasing from Ta to Nb and then to V, the phonon bandgap of "$k_{TaN}$–$m_{XN}$" decreases monotonously as indicated by the phonon dispersion in Figs. 2(g)–2(i).

Since the phonon bandgap can be modified significantly by changing mass of *X*, then, its effects on the thermal conductivity are calculated and shown in Fig. 4(a). If only three-phonon process is considered, "$k_{VN}$–$m_{TaN}$", "$k_{NbN}$–$m_{TaN}$", and "$k_{TaN}$–$m_{TaN}$", *i.e.*, fixed $m_{TaN}$, have the similar thermal conductivity especially around and above room temperature, suggesting that force constant has a weak effect on the thermal conductivity. On the other hand, for fixed $k_{TaN}$, *i.e.*, "$k_{TaN}$–$m_{TaN}$", "$k_{TaN}$–$m_{NbN}$", and "$k_{TaN}$–$m_{VN}$", the thermal conductivity has much different values. For example, at room temperature "$k_{TaN}$–$m_{TaN}$" has the largest thermal conductivity (1841 W/m·K) while "$k_{TaN}$–$m_{NbN}$" (199 W/m·K) and "$k_{TaN}$–$m_{VN}$" (250 W/m·K) have similar but much smaller thermal conductivity, suggesting that mass has a significant effect on

the thermal conductivity. In addition, we also calculate the thermal conductivities of "$k_{VN}$–$m_{VN}$" and "$k_{NbN}$–$m_{NbN}$", verifying the significant effects of mass and weak effects of force constant. Since the force constant has a weak effect on the thermal conductivity, the much smaller thermal conductivities of "$k_{VN}$–$m_{VN}$", "$k_{NbN}$–$m_{NbN}$", "$k_{TaN}$–$m_{NbN}$", and "$k_{TaN}$–$m_{VN}$" compared to those of "$k_{VN}$–$m_{TaN}$", "$k_{NbN}$–$m_{TaN}$", and "$k_{TaN}$–$m_{TaN}$" indicate that mass modified phonon bandgap has a significant effect on the thermal conductivity if only three-phonon process is considered.

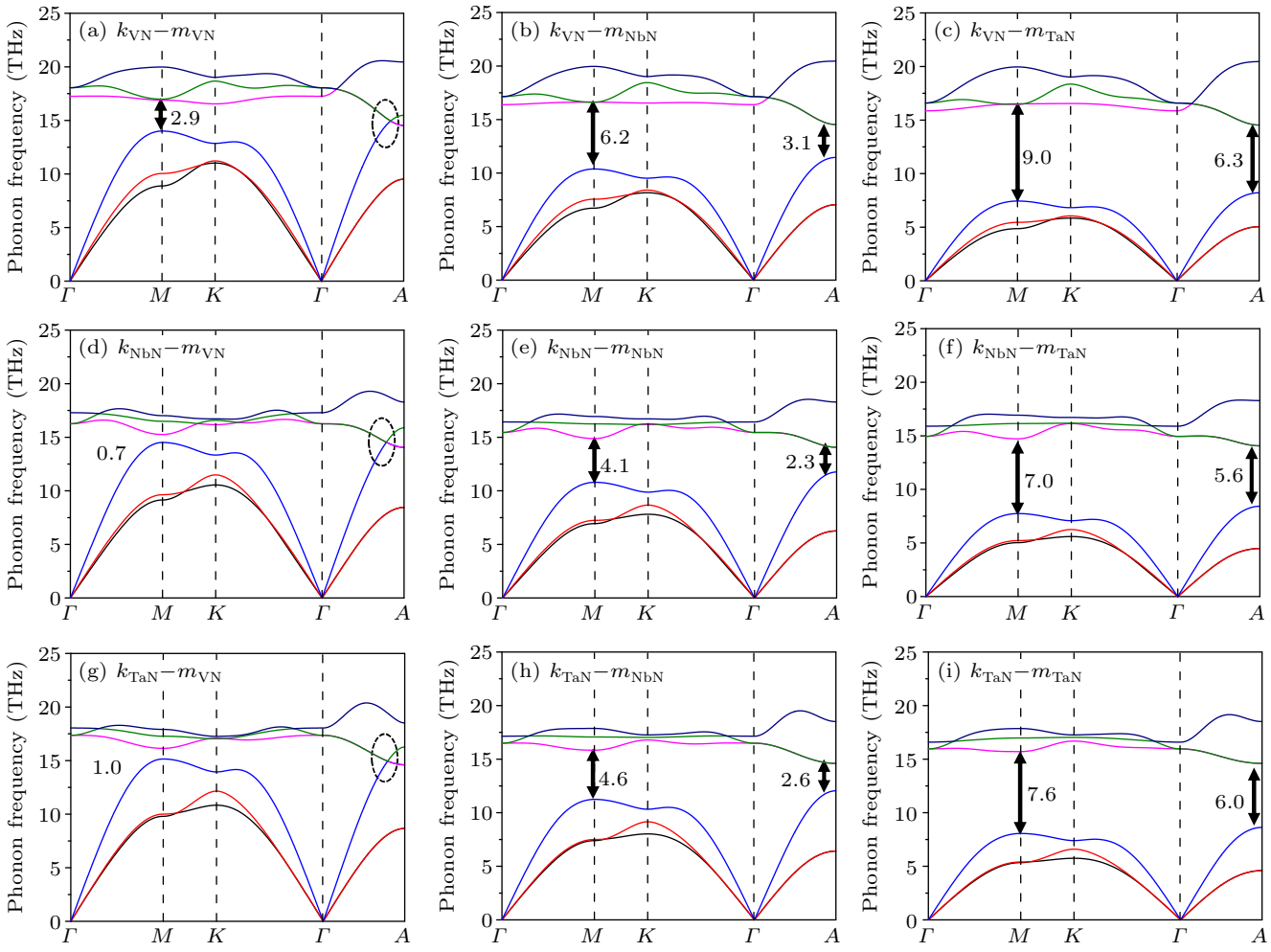



**Fig. 2.** Phonon dispersion of *X*N. The symbols in panels (a)–(i) mean the force constant and mass. For example, "$k_{VN}$–$m_{TaN}$" in panel (c) means the force constant of VN and mass of TaN are used to calculate the phonon dispersion. The numbers in panels (a)–(i) indicate the phonon bandgap and the unit is in THz.

When four-phonon process is introduced, the thermal conductivity of "$k_{TaN}$–$m_{TaN}$" has a significant drop. For example, its value decreases significantly from 1841 W/m·K to 957 W/m·K at room temperature. However, the thermal conductivities of "$k_{TaN}$–$m_{NbN}$" and "$k_{TaN}$–$m_{VN}$" only have a slight decrease. The reason for the significant drop and the slight decrease is that "$k_{TaN}$–$m_{TaN}$" has a large phonon bandgap while "$k_{TaN}$–$m_{NbN}$" and "$k_{TaN}$–$m_{VN}$" have a much smaller phonon bandgap. For a large phonon bandgap, although the three-phonon process is limited, the four-phonon process becomes allowed, causing the significant decrease of thermal conductivity in "$k_{TaN}$–$m_{TaN}$". For a small phonon bandgap, both three-phonon and four-phonon processes are allowed, thus the thermal conductivity has a slight drop in "$k_{TaN}$–$m_{NbN}$" and "$k_{TaN}$–$m_{VN}$" since the three-phonon process typically is much stronger than the four-phonon process.

Based on kinetic theory, thermal conductivity is determined by specific heat, phonon velocity, and phonon lifetime. In order to further investigate the effects of phonon bandgap on thermal conductivity, we will explore these three parameters in *X*N individually. For the first parameter of specific heat, its relationship is identical with mass. In other words, the mass is lighter, the specific heat is smaller, *i.e.*, $c(m_{VN}) < c(m_{NbN}) < c(m_{TaN})$. In *X*N, the acoustic phonon branches are dominated by *X* atom. When *X* is lighter, the maximum phonon frequency of acoustic phonons is larger and the phonon DOS has a red shift, leading to less active phonons below Debye temperature. Thus, specific heat is smaller for lighter *X*. When temperature is high enough, all phonons are activated and the mass of *X* cannot affect the specific heat, because in this case the specific heat is determined by the atom density based on Dulong–Petit law.[29] The much closer spe-

cific heat for different $X$ at higher temperature verifies the conclusion. Although specific heat has some difference due to the $X$-induced phonon bandgap, the difference is smaller than 10% at room temperature, which cannot explain the large difference of thermal conductivity such as the 7.4-fold difference of thermal conductivity between "$k_{TaN}$–$m_{TaN}$" and "$k_{TaN}$–$m_{VN}$" or the 10.9-fold difference of thermal conductivity between "$k_{TaN}$–$m_{TaN}$" and "$k_{VN}$–$m_{VN}$" (Fig. 3(a)).

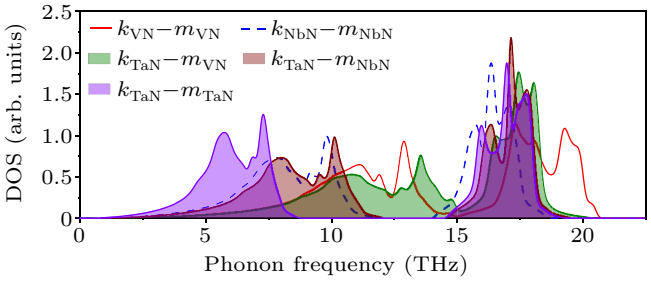



**Fig. 3.** Phonon density of states (DOS) of $X$N.

Then the phonon group velocity in XN is discussed. As shown in Figs. 4(c) and 4(d), the mode dependent phonon velocity has a significant change for fixed force constant while only has a slight change for fixed mass, which is similar to mass and force constant-dependent phonon dispersion and thermal conductivity shown above. For the case of fixed force constant, due to the largest mass of Ta, the phonon group velocity of "$k_{TaN}$–$m_{TaN}$" is smallest compared with "$k_{TaN}$–$m_{NbN}$" and "$k_{TaN}$–$m_{VN}$", which is inconsistent with its largest thermal conductivity. Since the phonon group velocity in Figs. 4(c) and 4(d) is mode-dependent, in order to distinctly and intuitively show the effects of phonon group velocity on thermal conductivity, the specific heat averaged phonon group velocity is calculated as follows:

$$\bar{P} = \frac{\sum_\lambda C_\lambda P_\lambda}{\sum_\lambda C_\lambda}, \tag{1}$$

where $P$ means the group velocity $v$ and $\lambda$ is the phonon mode. From the specific heat averaged phonon velocity (Table 2), "$k_{TaN}$–$m_{TaN}$" has the smallest $\bar{v}$. Thus, the phonon bandgap-dependent thermal conductivity in $X$N can only be explained by the phonon bandgap-dependent phonon lifetime or phonon–phonon scattering rates.

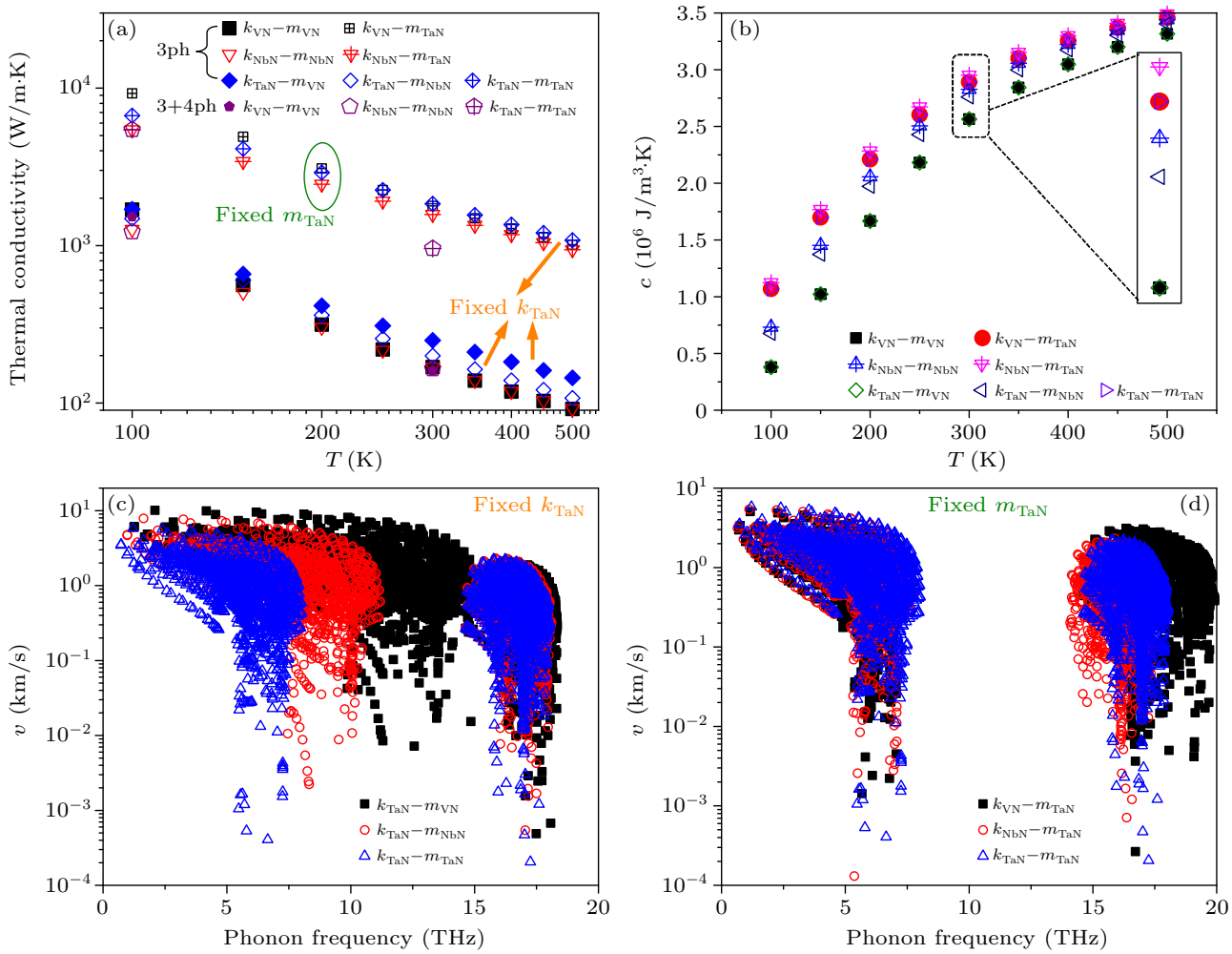



**Fig. 4.** (a) Temperature-dependent thermal conductivity in $X$N. "3ph" and "3 + 4ph", respectively, means the only three-phonon process and both the three-phonon and four-phonon processes for thermal conductivity calculation. "Fixed $m_{TaN}$" means the case for "$k_{VN}$–$m_{TaN}$", "$k_{NbN}$–$m_{TaN}$", and "$k_{TaN}$–$m_{TaN}$", while "Fixed $k_{TaN}$" means the case for "$k_{TaN}$–$m_{VN}$", "$k_{TaN}$–$m_{NbN}$", and "$k_{TaN}$–$m_{TaN}$". (b) Temperature–dependent specific heat in $X$N. Phonon frequency-dependent phonon group velocity for "Fixed $m_{TaN}$" (c) and "Fixed $k_{TaN}$" (d).

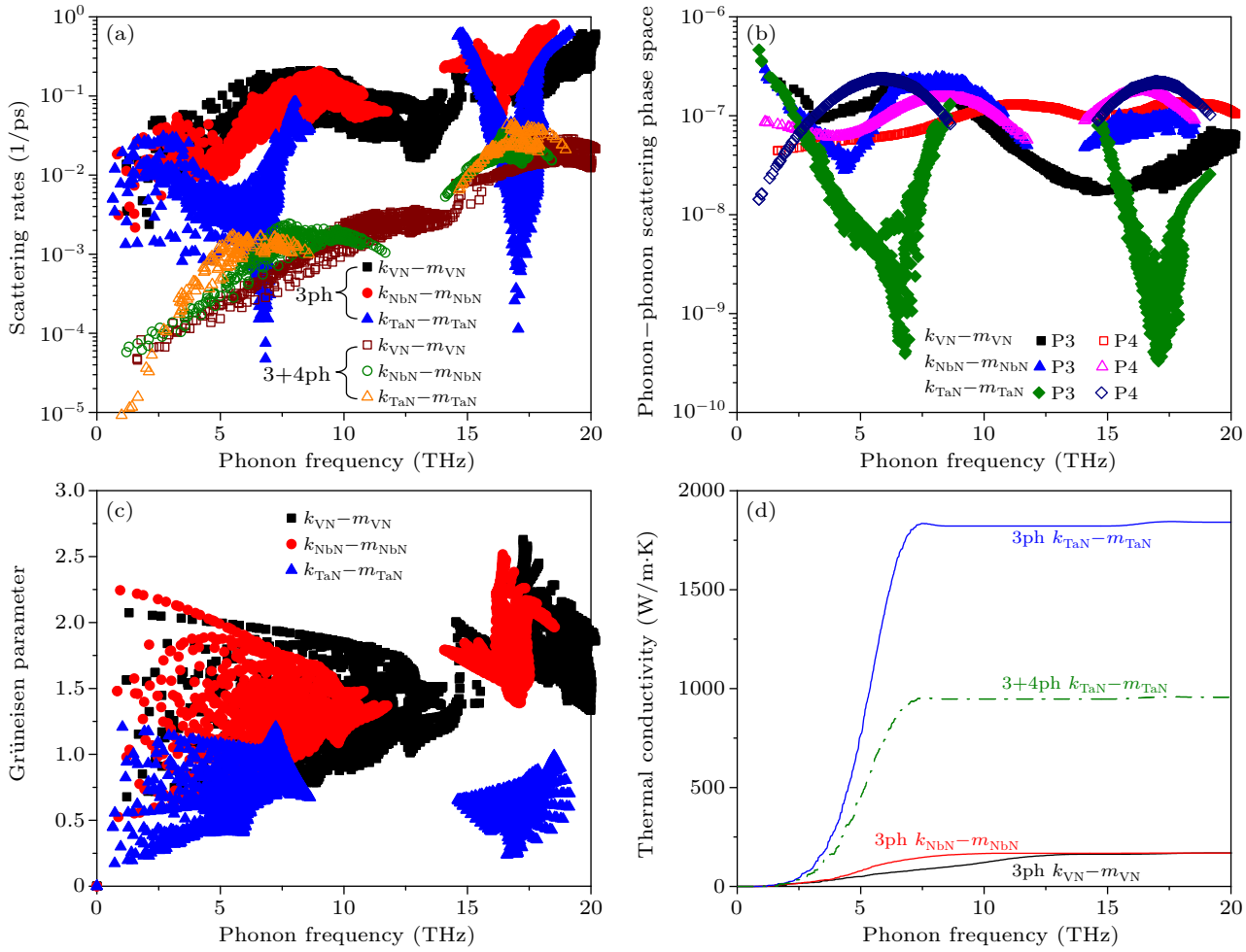



**Fig. 5.** Phonon frequency-dependent phonon–phonon scattering rates (a), scattering phase space (b), Grüneisen parameter (c), and cumulative thermal conductivity (d) in *X*N.

Figure 5(a) shows the phonon bandgap-dependent phonon–phonon scattering rates. Notably, since phonon bandgap and thermal conductivity have a weak dependence on force constant in *X*N, only "$k_{VN}$–$m_{VN}$", "$k_{NbN}$–$m_{NbN}$", and "$k_{TaN}$–$m_{TaN}$" are calculated to show the phonon bandgap effects. For "$k_{VN}$–$m_{VN}$" and "$k_{NbN}$–$m_{NbN}$", the mode dependent phonon–phonon scattering rate for three-phonon process is much larger than that for four-phonon process, which is reasonable since only a small phonon bandgap exist in the two materials. On the other hand, for "$k_{TaN}$–$m_{TaN}$", the mode dependent phonon–phonon scattering rate for three-phonon process is much smaller and within some frequency range the four-phonon process even has a stronger scattering, which are originated from the large phonon bandgap. The much smaller phonon–phonon scattering rate is the dominant reason for the ultrahigh thermal conductivity of "$k_{TaN}$–$m_{TaN}$". Since phonon–phonon scattering rate is determined by phonon–phonon scattering phase space and phonon anharmonicity, then the mode dependent P3, P4, and Grüneisen parameter are compared. For the phonon–phonon scattering phase space (Fig. 5(b)), similar to phonon–phonon scattering rates, phonon bandgap has a significant effect on P3 but a weak effect on P4. Specifically, the mode-dependent P4 for all three materials, *i.e.*, "$k_{VN}$–$m_{VN}$", "$k_{NbN}$–$m_{NbN}$", and "$k_{TaN}$–$m_{TaN}$", are similar, independent of phonon bandgap; while for the mode-dependent P3, "$k_{TaN}$–$m_{TaN}$" has much smaller value than that of "$k_{VN}$-$m_{VN}$" and "$k_{NbN}$–$m_{NbN}$" due to the large phonon bandgap. One the other hand, for the Grüneisen parameter (Fig. 5(c)), "$k_{TaN}$–$m_{TaN}$" has the smallest value, indicating the weak phonon anharmonicity. Thus, the ultrahigh thermal conductivity in "$k_{TaN}$–$m_{TaN}$" is caused by the weak phonon anharmonicity and large phonon bandgap induced weak phonon–phonon scattering strength.

Since the mode-dependent value is not that intuitive to present the phonon bandgap-dependent phonon–phonon scattering and thermal conductivity, then using Eq. (1), the specific heat averaged three-phonon lifetime $\tau_{3ph}$, four-phonon lifetime $\tau_{4ph}$, P3, P4, Grüneisen parameter, and phonon group velocity $v$ at room temperature are calculated and shown in Table 2. From the table, it is very clear that it is the long phonon lifetime ($\tau_{3ph}$ and $\tau_{4ph}$) and weak phonon anharmonicity (Grüneisen parameter) that dominates the ultrahigh thermal conductivity of "$k_{TaN}$–$m_{TaN}$", *i.e.*, TaN, since the specific heat has a weak effect on thermal conductivity and

phonon group velocity of "$k_{TaN}$–$m_{TaN}$" is the smallest. Finally, the phonon frequency cumulative thermal conductivities for "$k_{VN}$–$m_{VN}$", "$k_{NbN}$–$m_{NbN}$", and "$k_{TaN}$–$m_{TaN}$" are calculated. From Fig. 5(d), the saturated frequency for thermal conductivity is consistent with the maximum frequency of acoustic phonons, indicating that acoustic phonons dominate the thermal conductivity in *X*N.

**Table 2.** Thermal conductivity for three-phonon process ($\kappa_{3ph}$, in unit W/m·K) and four-phonon process ($\kappa_{4ph}$, in unit W/m·K), specific heat averaged phonon lifetime for three-phonon process ($\tau_{3ph}$, in unit ps) and four-phonon process ($\tau_{4ph}$, in unit ps), phonon–phonon scattering phase space for three-phonon process (P3) and four-phonon process (P4), Grüneisen parameter, and phonon velocity $v$ (in units km/s), and specific heat $C$ (in units J/m$^3$·K) at room temperature.

| | $\tau_{3ph}$ | $\tau_{4ph}$ | P3 ($10^{-8}$) | P4 ($10^{-8}$) | Grüneisen parameter | $C$ ($10^6$) | $v$ | $\kappa_{3ph}$ | $\kappa_{4ph}$ |
|---|---|---|---|---|---|---|---|---|---|
| VN | 12.5 | 603 | 6.30 | 11.7 | 1.51 | 2.56 | 1.13 | 169 | 161 |
| NbN | 12.8 | 754 | 13.5 | 14.2 | 1.50 | 2.83 | 0.94 | 169 | 165 |
| TaN | 187 | 1206 | 1.17 | 19.8 | 0.686 | 2.89 | 0.75 | 1841 | 957 |

## 3. Conclusion

In this work, the phonon bandgap effects on the phonon–phonon scattering and thermal conductivity in *X*N are investigated by first-principles calculations with linearized Boltzmann transport equation. Through comparing phonon dispersions in *X*N, mass has a significant effect on phonon bandgap while force constant has a weak effect. Through detailed calculations, it is found that the mass-induced phonon bandgap has a significant effect on phonon group velocity and phonon–phonon scattering phase space for three-phonon process while has a weak effect on specific heat and phonon–phonon scattering phase space for four-phonon process. The ultrahigh thermal conductivity of TaN is originated from the weak phonon–phonon scattering strength and phonon anharmonicity.

## Acknowledgments

Project supported by the National Natural Science Foundation of China (Grant No. 52206092) and the Natural Science Foundation of Jiangsu Province, China (Grant No. BK20210565). Liu C was funded by the Department of Science and Technology of Jiangsu Province (Grant No. BK20220032), the Basic Science (Natural Science) Research Project of Higher Education Institutions of Jiangsu Province, China (Grant No. 21KJB470009), Nanjing Science and Technology Innovation Project for Overseas Students, the "Shuangchuang" Doctor Program of Jiangsu Province, China (Grant No. JSSCBS20210315), and the Open Research Fund of Jiangsu Key Laboratory for Design and Manufacture of Micro-Nano Biomedical Instruments, Southeast University (Grant No. KF202010). The authors thank the Scientific Computing Center of Nanjing Normal University and the Big Data Center of Southeast University for performing the numerical calculations presented in this paper.

## References

[1] Kang J S, Li M, Wu H A, Nguyen H and Hu Y J 2018 *Science* **361** 575
[2] Li S, Zheng Q Y, Lv Y C, Liu X Y, Wang X Q, Huang P S E Y, Cahill D G and Lv B 2018 *Science* **361** 579
[3] Tian F, Song B, Chen X, Ravichandran N K, Lv Y C, Chen K, Sullivan S, Kim J, Zhou Y Y, Liu T H, Goni M, Ding Z W, Sun J Y, Gamage G A G U, Sun H R, Ziyaee H, Huyan S Y, Deng L Z, Zhou J S, Schmidt A J, Chen S, Chu C W, Huang P S E Y, Broido D, Shi L, Chen G and Ren Z F 2018 *Science* **361** 582
[4] Slack G A 1973 *J. Phys. Chem. Solids* **34** 321
[5] Balandin A A, Ghosh S, Bao W Z, Calizo I, Teweldebrhan D, Miao F and Lau C N 2008 *Nano Lett.* **8** 902
[6] Balandin A A. 2011 *Nat Mater.* **10** 569
[7] Wei L, Kuo P K, Thomas R L, Anthony T R and Banholzer W F 1993 *Phys. Rev. Lett.* **70** 3764
[8] Onn D G, Witek A, Qiu Y Z, Anthony T R and Banholzer W F 1992 *Phys. Rev. Lett.* **68** 2806
[9] Inyushkin A V, Taldenkov A N, Ralchenko V G, Bolshakov A P, Koliadin A V and Katrusha A N 2018 *Phys. Rev. B* **97** 144305
[10] Lindsay L, Broido D A and Reinecke T L 2013 *Phys. Rev. Lett.* **111** 025901
[11] Dames C. 2018 *Science* **361** 549
[12] Liu C H, Chen Z H, Wu C, Qi J, Hao M L, Lu P and Chen Y F 2022 *ACS Appl. Mater. Inter.* **14** 46716
[13] Vega-Flick A, Jung D, Yue S Y, Bowers J E and Liao B L 2019 *Phys. Rev. Mater.* **3** 034603
[14] Yang R Q, Yue S Y, Quan Y J and Liao B L 2021 *Phys. Rev. B* **103** 184302
[15] Liu C, Wu C, Song T, Zhao Y, Yang J, Lu P, Zhang G and Chen Y 2022 *ACS Appl. Energy Mater.* **5** 15356
[16] Kundu A, Yang X L, Ma J L, Feng T L, Carrete J, Ruan X L, Madsen G K H and Li W 2021 *Phys. Rev. Lett.* **126** 115901
[17] Feng T L and Ruan X L 2018 *Phys. Rev. B.* **97** 045202
[18] Gu X K, Fan Z Y, Bao H and Zhao C Y 2019 *Phys. Rev. B.* **100** 064306
[19] Liu C H, Lu P, Chen W Y, Zhao Y S and Chen Y F 2021 *Phys. Chem. Chem. Phys.* **23** 26030
[20] Li W, Carrete J, Katcho N A and Mingo N 2014 *Comput. Phys. Commun.* **185** 1747
[21] Liu C, Lu P, Gu Z, Yang J and Chen Y 2020 *J. Phys. Chem. C* **124** 26144
[22] Liu C, Mishra V, Chen Y and Dames C 2018 *Adv. Theory Simul.* **1** 1800098
[23] Liu C, Chen Y and Dames C 2019 *Phys. Rev. Appl.* **11** 044002
[24] Liu C, Lu P, Li D, Zhao Y and Hao M 2022 *Mater. Today Nano* **17** 100165
[25] Liu C and Chen Y 2022 *Sci. China Phys. Mech.* **65** 117009
[26] Bai S Y, Tang Z A, Huang Z X, Yu J and Wang J Q 2008 *Chin. Phys. Lett.* **25** 593
[27] Li H L and Cao B Y 2019 *Acta Phys. Sin.* **68** 200201 (in Chinese)
[28] Friedrich A, Winkler B, Bayarjargal L, Arellano E A J, Morgenroth W, Biehler J, Schroder F, Yan J Y and Clark S M 2010 *J. Alloys Compd.* **502** 5
[29] Fitzgerel R K and Verhoek F H 1960 *J. Chem. Educ.* **37** 545